

Received January 31, 2021, accepted February 14, 2021, date of publication February 22, 2021, date of current version March 1, 2021.

Digital Object Identifier 10.1109/ACCESS.2021.3061099

Filtering Quasi-Yagi Strip-Loaded DRR Antenna With Enhanced Gain and Selectivity by Metamaterial

YAN-HUI KE^{1,2}, LING-LING YANG^{1,2,3}, YAN-YUAN ZHU⁴, JIANPENG WANG^{1,4},
AND JIAN-XIN CHEN^{1,2,5}, (Senior Member, IEEE)

¹School of Electronics and Information, Nantong University, Nantong 226019, China

²Research Center for Intelligent Information Technology, Nantong University, Nantong 226019, China

³Xinglin College, Nantong University, Nantong 226019, China

⁴Ministerial Key Laboratory of JGMT, Nanjing University of Science and Technology, Nanjing 210094, China

⁵Nantong Research Institute for Advanced Communication Technologies, Nantong 226019, China

Corresponding author: Jian-Xin Chen (jjxchen@hotmail.com)

This work was supported in part by the National Natural Science Foundation of Jiangsu under Grant BK20201438, and in part by the Natural Science Research Project of Jiangsu Provincial Institutions of Higher Education under Grant 20KJA510002 and Grant 20KJB510010.


ABSTRACT This paper presents a design approach of broadband filtering quasi-Yagi DRR Antenna using a strip-loaded dielectric ring resonator (DRR) and near-zero-index (NZI) metamaterial (NZIM). The ring strip is loaded to the inside wall of the DRR so that the $TE_{01\delta}$ and $TE_{21\delta}$ modes of the DRR can be close. Meanwhile, they function as a dual-mode magnetic dipole (M-dipole) driver and can be differentially excited at the same time for designing a wideband quasi-Yagi antenna. Benefiting from the dual-mode operation of the strip-loaded DRR, the end-fire gain across the operating band of the antenna is stable with preliminary bandpass filtering characteristics. To improve the in-band gain and enhance the filtering capability, a new coplanar NZIM with wideband NZI characteristic and dual transmission notches in the lower and upper stopbands of the preliminary gain passband, is introduced and put in the front of the DRR driver. To verify the proposed design concept, an X-band filtering quasi-Yagi antenna with the NZIM is fabricated and measured. Good agreement between the simulated and measured results can be observed. The wideband antenna has a measured -10 dB impedance bandwidth of about 16% (8.5 – 10 GHz). Within it, the peak gain of antenna reaches 8.3 dBi and 1-dB gain fractional bandwidth is about 10.8%. Meanwhile, it exhibits good gain bandpass response due to the transmission notches of the NZIM.

INDEX TERMS Quasi-Yagi antenna, filtering antenna, dielectric ring resonator (DRR), near-zero-index (NZI) metamaterial (NZIM).

I. INTRODUCTION

With the rapid development of wireless communication systems, various end-fire antennas have drawn extensive attentions due to their high gain and good directivity. In among, the quasi-Yagi antenna is particularly prominent on account of its advantages, such as light weight, simple structure, and easy forming arrays [1]–[4]. But it usually has a narrow operating band, which could not meet the multi-frequency operation requirements of wireless communication. Accordingly, lots of efforts have been made to enlarge the impedance bandwidth. In [5], a bowtie driver is adopted to improve the

impedance matching. In [6]–[8], the wideband feeding baluns are adopted to enlarge impedance bandwidth of the antenna, but the gain fluctuation is large and in the low frequency range it is only about 4 dBi. The reason mainly includes two factors: 1) The driver is one-mode operation and is not able to provide good wideband radiation. 2) The director is also not able to provide wideband gain enhancement [6]. To solve this problematic issue, multiple series dipoles with different resonant frequencies are fed, and both wide bandwidth and stable moderate gain can be obtained [9]–[11]. Nevertheless, the longitudinal length is increased significantly while further gain improvement in the wide bandwidth is still difficult and becomes a challenging work. Recently, the microstrip magnetic dipole (M-dipole) has been presented, and the

The associate editor coordinating the review of this manuscript and approving it for publication was Chinmoy Saha .

fundamental TE_{110} mode is shifted up by adding the shorting via and is close to the higher-order TE_{310} mode [12]. The enhanced bandwidth due to the combination of two modes is achieved. However, the transverse size of the driver reaches $1.5\lambda_0$, where λ_0 is the free-space wavelength at the center frequency.

The dielectric resonator (DR), as a good radiator, has been widely applied in the designs of various antennas due to high radiation efficiency and flexible structure [13]–[18] in the past decades. Recently, it is used as an M-dipole [19] for designing a quasi-Yagi antenna. In [20], a quasi-Yagi antenna using a rectangular DR (RDR) is reported, showing higher gain over traditional metallic quasi-Yagi antenna. The end-fire gain can be further enhanced by adding proper RDR or strip directors in the front of RDR driver. However, it has a narrow bandwidth of about 3% since only one $TE_{1\delta 1}$ mode is adopted. In [21], the $TE_{1\delta 1}$ and $TE_{1\delta 3}$ modes of the RDR are controlled by varying the length-to-width ratio for designing dual-band quasi-Yagi antenna. By properly adding directors with different sizes, which bring extra resonances between the two modes, the wideband antenna comes into being. However, time-consuming optimization is required to balance the wideband impedance matching and gain enhancement. In [22], a cylinder DR M-dipole is combined with the folded strip electric dipole (E-dipole) on the opposite side of the substrate for designing bandwidth-enhanced quasi-Yagi antenna, which would be difficult for implementation of two-dipole alignment. The in-band gain is evenly improved by adding the near-zero-index (NZI) metamaterial (NZIM) in the front of them because the NZIM can provide broadband NZI characteristic [23]–[25]. However, thus far, all of the existing quasi-Yagi DR antennas have not considered the integration of filtering function.

In the past few years, filtering antenna has become a hot topic in the microwave field and has attracted much attention, which can replace the cascaded antennas and filter to reduce size and loss [26]–[28]. Accordingly, filtering quasi-Yagi antenna has been developed recently [29]–[33], and the design method depends on embedding the filtering balun with bandpass response into the feeding network. However, the potential mentioned above of filtering-antenna fusion design has not been realized entirely.

In this paper, a broadband filtering quasi-Yagi antenna using strip-loaded dielectric ring resonator (DRR) is proposed. The $TE_{01\delta}$ and $TE_{21\delta}$ modes of the DRR are designed in close frequency spacing and can be used as a dual-mode driver for designing bandwidth-enhanced quasi-Yagi antenna with stable in-band gain. Meanwhile, its gain shows a preliminary bandpass filtering response. To improve filtering antenna performance, a new coplanar NZIM structure is proposed and put in the front of the DRR driver, which is different from traditional NZIMs with one function of NZI [22]–[25]. It provides two functions, i.e. one is to improve the in-band gain by using the wideband NZI characteristic, and the other is to enhance the filtering selectivity by introducing dual transmission notches in the lower and upper stopbands of

the preliminary gain passband. For demonstration, an X-band filtering quasi-Yagi antenna with the NZIM is designed, fabricated and measured. Good agreement between the simulated and measured results can be observed.

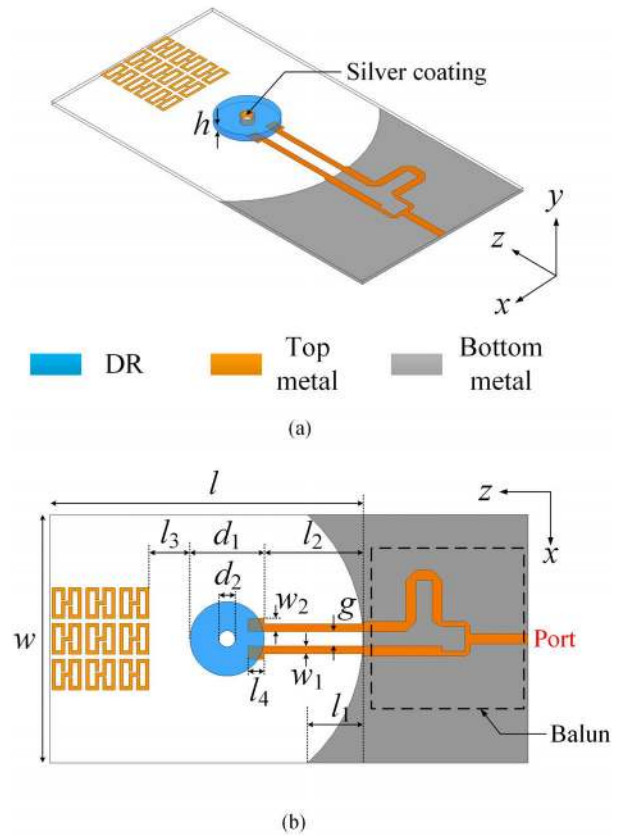


FIGURE 1. Configuration of proposed filtering quasi-Yagi antenna with the NZIM, (a) 3-D view, (b) top view. ($l = 36.7$ mm, $w = 30$ mm, $l_1 = 19$ mm, $l_2 = 12$ mm, $l_3 = 5$ mm, $l_4 = 2.3$ mm, $w_1 = 0.9$ mm, $w_2 = 1.6$ mm, $d_1 = 9$ mm, $d_2 = 2$ mm, and $h = 1$ mm.)

II. DESIGN OF THE PROPOSED BROADBAND FILTERING QUASI-YAGI ANTENNA

Fig. 1 shows the configuration of the proposed broadband filtering quasi-Yagi DRR antenna using the strip-loaded DRR on the top of a substrate ($l \times w$) and the coplanar NZIM in the front of it. The DRR ($\epsilon_{r1} = 38$ and $\tan\delta = 0.0015$) is constructed by penetrating a central hole in the traditional cylinder DR, and the inside wall of the hole is coated by a ring silver strip. The substrate is Rogers 4003C laminate with a dielectric constant of $\epsilon_{r2} = 3.38$ and a loss tangent of $\tan\delta = 0.0027$. The DRR is differentially fed through the coplanar strip line (CPS) on the top of the substrate. The arc-shaped ground plane on the bottom of the substrate is used as a reflector for achieving end-fire radiation.

A. STRIP-LOADED DRR

It is well known that the $TE_{01\delta}$ mode is the dominant one of the cylinder DR ($d_2 = 0$ mm in Fig. 1), and its electric-field (E-field) circulates azimuthally and tangential to the x-z plane, as shown in Fig. 2 (a). Meanwhile, the $TE_{01\delta}$ mode

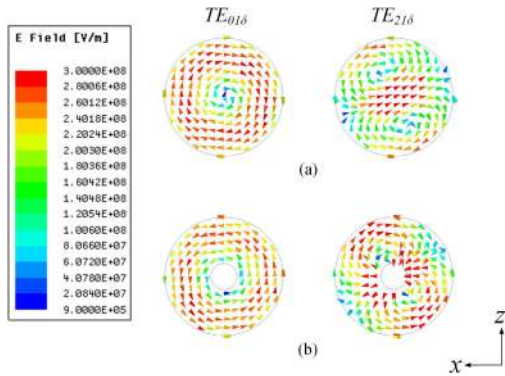


FIGURE 2. E-field of Cylinder DR and strip-loaded DRR, (a) Cylinder DR, (b) strip-loaded DRR.

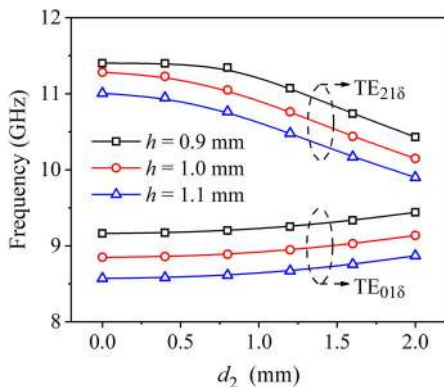


FIGURE 3. The frequencies of $TE_{01\delta}$ and $TE_{21\delta}$ modes under different d_2 . ($d_1 = 9$ mm and $\epsilon_{r1} = 38$ are fixed).

E-field density at the center of the DR is lowest. Therefore, the strip-loaded hole placed at the center of DR doesn't have much effect on the $TE_{01\delta}$ mode. The $TE_{21\delta}$ mode is the lowest-frequency high-order mode, and its E-field is also tangential to the x-z plane. Unlike the $TE_{01\delta}$ mode, the E-field of the $TE_{21\delta}$ is concentrated in the center of the DR, which means the strip-loaded hole here is equivalent to an electric wall located in the path of the E-field. It can be expected that loading a sliver-coated hole at the center of the cylinder DR has small effect on the dominant $TE_{01\delta}$ mode while has significant effect on the high-order $TE_{21\delta}$ mode of the DRR, which can be confirmed by the change of E-field distributions shown in Fig. 2 (b). Fig. 3 shows the resonant frequencies of $TE_{01\delta}$ and $TE_{21\delta}$ modes against the hole diameter d_2 under different thickness h of the strip-loaded DRR. As d_2 increases, the $TE_{21\delta}$ mode frequency shifts down dramatically while the $TE_{01\delta}$ mode frequency increases gradually. As a result, when the strip-loaded hole is incorporated, they can be designed in a close spacing and combined together to achieve a wideband design of the antenna.

B. BASIC ANTENNA

According to the above analysis, the strip-loaded DRR can be used as a dual-mode M-dipole (both along y-axis direction) operating at two close frequencies to design a bandwidth-enhanced quasi-Yagi antenna. Here the NZIM and balun in Fig. 1 are not included for building a basic antenna. To excite

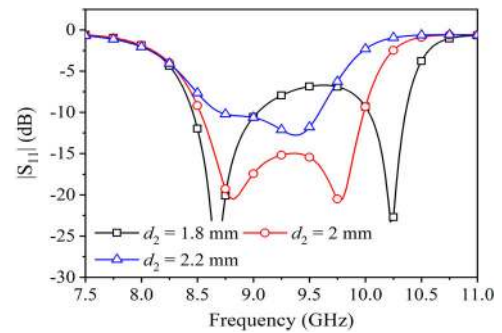


FIGURE 4. Simulated $|S_{11}|$ of proposed basic antenna under different d_2 . ($d_1 = 9$ mm, $h = 1$ mm and $\epsilon_{r1} = 38$ are fixed).

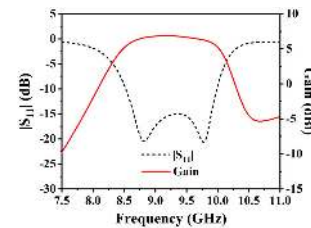


FIGURE 5. Simulated $|S_{11}|$ and gain of basic antenna without the NZIM and balun.

the two modes at the same time, the balanced transmission line, i.e. the CPS is applied because the E-field distribution of the CPS (parallel to the x-z plane) is consistent with those of the two modes [20]. Under this condition, the CPS is designed to be stepped-width, and the parameters w_1 , w_2 and g_2 can be tuned to achieve good impedance matching in a broad band.

Fig. 4 shows the simulated reflection coefficient ($|S_{11}|$) under different d_2 . As expected, the $TE_{21\delta}$ mode (corresponding to the upper resonant frequency) shifts down while the $TE_{01\delta}$ mode (corresponding to the lower resonant frequency) shifts up slightly, which is well consistent with the variation trend shown in Fig. 3. To design a wideband quasi-Yagi antenna, we choose $d_2 = 2$ mm for good impedance matching. The simulated $|S_{11}|$ and gain of the basic antenna is presented in Fig. 5. The fractional bandwidth (FBW) for $|S_{11}| < -10$ dB is about 16 % (8.5 - 10 GHz). In the operating band, the end-fire peak gain is up to 6.3 dBi, which is about 1-dB higher than that of the quasi-Yagi antenna using the strip E-dipole with one director [32], [33]. Fig. 6 depicts the simulated radiation patterns in both E- and H-planes at 8.75 GHz and 9.75 GHz. As can be seen from Fig. 5, both high stable gain in a broad band (due to dual-mode radiation) and preliminary filtering response can be observed. However, its filtering selectivity is not adequate, especially in the upper stopband. In this case, we apply the dual-notch NZIM as follows instead of traditional metal strip director [21] to improve the selectivity.

C. DESIGN OF THE DUAL-NOTCH NZIM

In this section, a new coplanar NZIM structure with dual transmission notches is designed to achieve two targets: One is to entirely enhance the gain in the whole operating band by using the wideband NZI characteristic of the NZIM, and the other is to improve the out-of-band suppression by

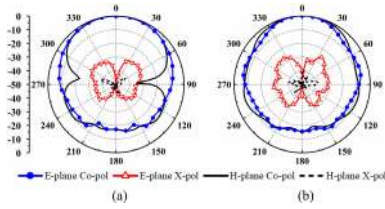


FIGURE 6. Simulated radiation patterns of basic antenna without the NZIM, (a) 8.75 GHz, (b) 9.75 GHz.

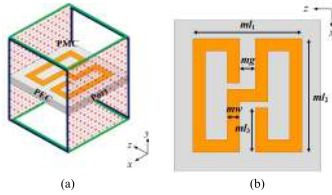


FIGURE 7. Configuration of the proposed NZIM unit cell, (a) 3-D view of simulation model, (b) Top view. ($m_{l1} = 3.5$ mm, $m_{l2} = 3.7$ mm, $m_{l3} = 1.45$ mm, $m_w = 0.4$ mm, and $m_g = 0.5$ mm).

introducing the radiation nulls of the lower and upper gain stopbands resulting from the dual notches of the NZIM. Fig. 7 (a) shows the simulation model of the NZIM unit cell printed on the top of the substrate, and its dimensions are given in Fig. 7 (b). Since the incident wave propagating along z-direction with x-direction polarization is the main interest, which is consistent with the end-fire radiation of the proposed quasi-Yagi antenna shown in Fig. 1. The simulation setup is as follows. The two ports are perpendicular to the propagating z-direction. The two surfaces of the waveguide, perpendicular to x-direction, are assigned as perfect electric conducting (PEC) and the other two sides as perfect magnetic conducting (PMC).

The dual-notch frequencies (f_{n1} and f_{n2}) are mainly determined by the total length of the strip, while they can be tuned by other parameters of the unit cell. Fig. 8 (a) shows the transmission coefficient ($|S_{21}|$) under strip width m_w , where the total length of the strip remains unchanged. Both f_{n1} and f_{n2} move down as m_w decreases (implying the inductance of the unit cell increases). Besides, the ratio (f_{n2}/f_{n1}) of the dual-notch frequencies can be controlled by the parameters of m_g , m_w , and m_{l3} , which is flexible and helpful to design two notches at desired frequencies.

Fig. 9 shows the configuration of the NZIM array with three cascaded unit cells, which is used for the following antenna design and Fig. 10 shows the extracted refractive index (n) and $|S_{21}|$ under different distance d_y between the unit cells. As can be seen from Fig. 10(a), as d_y increases, the real part of n , i.e. $Re(n)$, increases in the frequency range of interest (8.5 to 10 GHz) while the imaginary part of n , i.e. $Im(n)$, becomes close to zero, implying lower loss introduced by the NZIM array, especially in higher frequency range. On the other hand, three sub-notch frequencies can be observed in either lower or upper notch band due to three NZIM unit cells in the array. Meanwhile, the distance d_y determines the coupling between the unit cells. As d_y decreases, meaning the coupling becomes strong, the sub-notch frequencies become far away in both notch bands, as shown in Fig. 10(b).

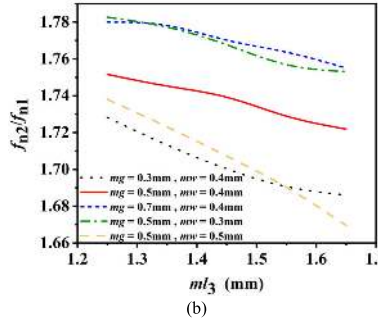
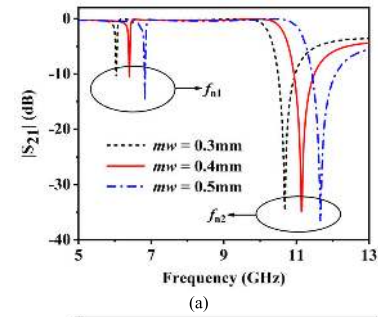


FIGURE 8. Simulated results of the NZIM unit cell, (a) Transmission coefficient under different m_w , (b) f_{n2}/f_{n1} against m_{l3} under different m_g and m_w .

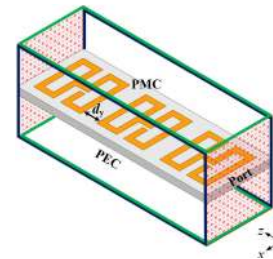


FIGURE 9. Simulation model of the NZIM array.

D. PROPOSED ANTENNA WITH THE NZIM

According to the above discussions, a broadband filtering quasi-Yagi antenna can be easily constructed by combing the basic antenna and the NZIM together. By optimization, the dimensions of the antenna are obtained and shown in Fig. 1 and Fig. 7. The distance $d_y = 0.6$ mm between the NZIM unit cells is chosen so that $Re(n)$ is from -1 to 0.4 and $Im(n)$ is lower than 0.5 in frequency range of 8.5-10 GHz. Meanwhile, the three sub-notches in each notch band are near to the gain passband so that the filtering selectivity can be improved significantly. Fig. 11 shows the simulated $|S_{11}|$ and gain of the antenna with/without the NZIM. It can be found that the NZIM has a rare effect on the bandwidth while the in-band gain is entirely improved by about 2 dB and keeps stable. Remarkably, the gain filtering response is improved significantly, especially in the upper stopband, where the suppression improvement reaches about 10dB. In addition, it can be seen from Fig. 11 that the distance l_3 between the NZIM and DRR cannot almost affect the antenna performance and the slight difference lies in the gain enhancement. This implies the basic antenna and NZIM can be independently designed, showing simplified design procedure. As l_3 increases, the gain enhancement is slightly enlarged. But it

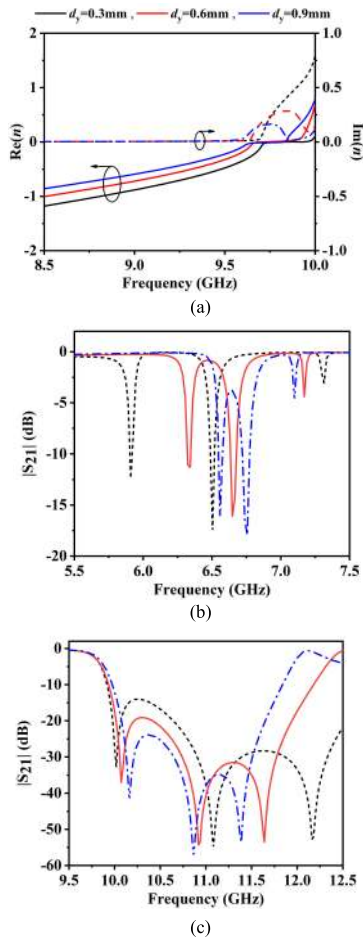


FIGURE 10. The simulated results of the NZIM array, (a) Refractive index (n), (b) transmission coefficient ($|S_{21}|$) in the lower notch band, and (c) $|S_{21}|$ in the upper notch band under different d_y .

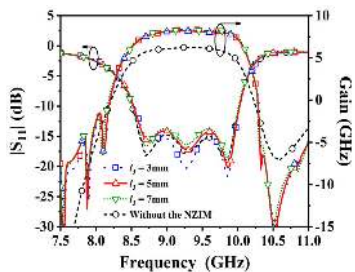


FIGURE 11. Comparison of $|S_{11}|$ and gain between the basic antenna without the NZIM and the proposed antenna with the NZIM under different l_3 .

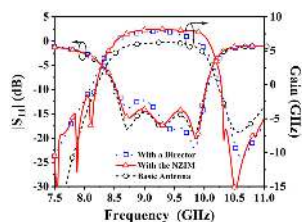


FIGURE 12. Comparison of $|S_{11}|$ and gain between basic antenna, antenna with metal strip director and antenna with the NZIM.

is inevitable that the antenna total length is enlarged as well. Therefore $l_3 = 5$ mm is chosen for the proposed antenna. In Fig. 12, we can clearly see the advantages of the proposed

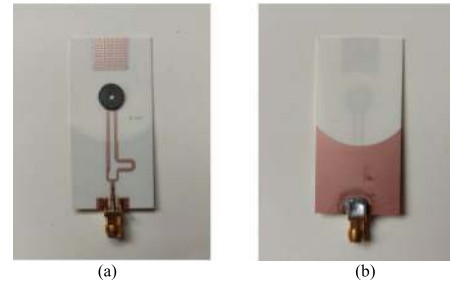


FIGURE 13. Photograph of the proposed filtering quasi-Yagi antenna. (a) Top view, and (b) bottom view.

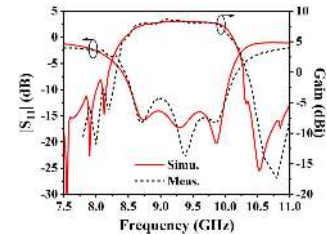


FIGURE 14. The simulated and measured $|S_{11}|$ and gain of the proposed filtering quasi-Yagi antenna with the NZIM.

TABLE 1. Performance comparison with previous filtering quasi-yagi antenna.

Ref	f_0 (GHz)	FBW (%)	Peak gain (dBi)	Size ($\lambda_0 \times \lambda_0$)	Radiation nulls	Design method
[29]	2.5	48	4.7	1×0.92	N/A	Complex
[30]	4.4	34.1	5.1	0.51×0.59	YES	Complex
[31]	3.96	18.5	5.8	0.45×0.83	YES	Complex
[32]	1.72	16.8	5.5	0.7×0.7	NO	Complex
[33]	1.82	5.5	5.6	0.61×0.36	NO	Complex
This work	9.25	16.2	8.5	0.94×1.1	YES	Simple

antenna with the NZIM over traditional RDR Yagi antennas with metal strip director [21]. One is the entire and stable gain enhancement in the whole band, given that traditional director can only provide 0.63 dB gain enhancement at 10 GHz, where the NZIM can provide 2.44 dB gain enhancement. The other is a good improvement in selectivity, as can be seen from Fig. 12.

III. VERIFICATION AND DISCUSSION

To verify the proposed design concept, a wideband filtering quasi-Yagi antenna using the strip-loaded DRR and NZIM is designed and fabricated. Fig. 13 shows the photographs of the implemented antenna with the NZIM, whose electrical size is $0.94\lambda_0 \times 1.1\lambda_0$. A microstrip balun based on the 180° delay line is designed to connect with the CPS for antenna test. Fig. 14 shows the simulated and measured $|S_{11}|$ and gain of proposed antenna, exhibiting good agreement. The measured impedance FBW ($|S_{11}| < -10$ dB) is about 16% from 8.5 to 10 GHz, and the measured peak gain is up to

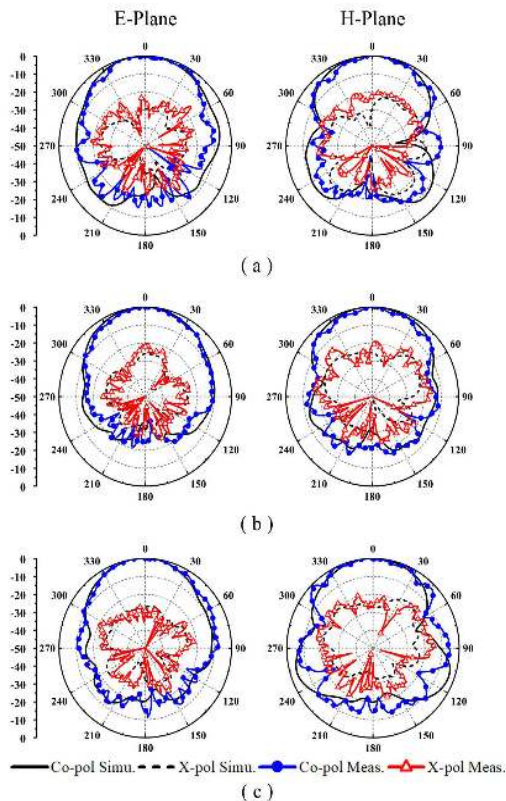


FIGURE 15. Simulated and measured radiation patterns of proposed filtering quasi-Yagi antenna with the NZIM, (a) 8.73 GHz, (b) 9.27 GHz, (c) 9.87 GHz.

8.3 dBi across in operating band and the 1-dB gain FBW is about 10.8% (from 8.9 to 9.9 GHz), showing stable in-band gain. Besides, the measured dual notches are also consistent with the simulated ones. Fig. 15 shows the simulated and measured radiation patterns in both E- and H-planes at 8.73 GHz, 9.27 GHz and 9.87 GHz, respectively. Their cross-polarization levels of less than -20 dB are observed within $\pm 30^\circ$ beam width. The front-to-back ratio is more than 10 dB in the whole operating band. The comparison of the proposed antenna with previous filtering quasi-Yagi antennas is summarized in Table 1. In [29]–[32], by adding different filtering structures into feeding network, several broadband filtering quasi-Yagi antennas are obtained. Although that's an effective method to obtain good filter response, complex feeding and extra loss structures are unavoidable. Therefore, the peak gains of these antennas with one director are low, ranging from 4.7 to 5.8 dBi, which is even lower than the basic antenna proposed in this paper. In [33], by inserting a double-sided parallel-strip line (DPSL) filter between the driver and the reflector, the proposed filtering quasi-Yagi antenna achieves frequency selectivity without increasing the overall size. However, the loss brought by the filtering structure is still a problem, resulting in peak gain of only 5.5 dBi. In this work, the proposed antenna has the highest gain due to the reasonable combination of dual-mode DRR driver and NZIM. Since the distance between the NZIM and DRR driver cannot affect the antenna performance while the incorporation of

the NZIM has rare effect on the impedance matching in a broad band, the design method is much simpler than those using the cascaded filter and antenna [29]–[32], where it is inevitable that the time-consuming optimization is required when cascading the two components.

IV. CONCLUSION

In this paper, a broadband filtering quasi-Yagi DRR antenna with enhanced gain and selectivity by the NZIM has been presented. The $TE_{01\delta}$ and $TE_{21\delta}$ modes of the DRR can be effectively excited at the same time and used as a dual-mode dipole. By introducing the NZIM with dual-notch in the front of strip-loaded DRR driver in a simple way, the in-band gain can be effectively enhanced and the out-of-band suppression can be improved simultaneously. The demonstration antenna has been designed and implemented, and the simulated and measured results with good accordance have been presented.

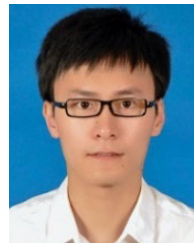
REFERENCES

- [1] D. Isbell, "Log periodic dipole arrays," *IRE Trans. Antennas Propag.*, vol. 8, no. 3, pp. 260–267, May 1960.
- [2] J. Liu and Q. Xue, "Microstrip magnetic dipole Yagi array antenna with endfire radiation and vertical polarization," *IEEE Trans. Antennas Propag.*, vol. 61, no. 3, pp. 1140–1147, Mar. 2013.
- [3] J. R. Brianeze, A. C. Sodré, Jr., and H. E. Hernández-Figueroa, "Tridimensional Yagi antenna: Shaping radiation pattern with a non-planar array," *IET Microw., Antennas Propag.*, vol. 4, no. 9, pp. 1434–1441, Sep. 2010.
- [4] T. Yang, D. Yang, and D. Geng, "Compact planar quasi-Yagi antenna with band-notched characteristic for WLAN and DSRC for ultra-wideband applications," *IET Microw., Antennas Propag.*, vol. 12, no. 7, pp. 1239–1245, Jun. 2018.
- [5] S. A. Rezaeieh, M. A. Antoniadis, and A. M. Abbosh, "Miniaturized planar Yagi antenna utilizing capacitively coupled folded reflector," *IEEE Antennas Wireless Propag. Lett.*, vol. 16, pp. 1977–1980, 2017.
- [6] J. Wu, Z. Zhao, Z. Nie, and Q.-H. Liu, "Design of a wideband planar printed quasi-Yagi antenna using stepped connection structure," *IEEE Trans. Antennas Propag.*, vol. 62, no. 6, pp. 3431–3435, Jun. 2014.
- [7] H. Chu, Y.-X. Guo, H. Wong, and X. Shi, "Wideband self-complementary quasi-Yagi antenna for millimeter-wave systems," *IEEE Antennas Wireless Propag. Lett.*, vol. 10, pp. 322–325, 2011.
- [8] J. Wu, Z. Zhao, Z. Nie, and Q.-H. Liu, "Bandwidth enhancement of a planar printed quasi-Yagi antenna with size reduction," *IEEE Trans. Antennas Propag.*, vol. 62, no. 1, pp. 463–467, Jan. 2014.
- [9] B.-K. Tan, S. Withington, and G. Yassin, "A compact microstrip-fed planar dual-dipole antenna for broadband applications," *IEEE Antennas Wireless Propag. Lett.*, vol. 15, pp. 593–596, 2016.
- [10] S. A. Rezaeieh, M. A. Antoniadis, and A. M. Abbosh, "Miniaturization of planar Yagi antennas using Mu-negative metamaterial-loaded reflector," *IEEE Trans. Antennas Propag.*, vol. 65, no. 12, pp. 6827–6837, Dec. 2017.
- [11] L. Yang, J. Zhang, and W. Wu, "Wideband microstrip series-fed magnetic dipole array antenna," *Electron. Lett.*, vol. 50, no. 24, pp. 1793–1795, Nov. 2014.
- [12] Y. Shi and J. Liu, "Investigation of a via-loaded microstrip magnetic dipole antenna with enhanced bandwidth and gain," *IEEE Trans. Antennas Propag.*, vol. 67, no. 7, pp. 4836–4841, Jul. 2019.
- [13] Y. M. Pan and S. Y. Zheng, "A low-profile stacked dielectric resonator antenna with high-gain and wide bandwidth," *IEEE Antennas Wireless Propag. Lett.*, vol. 15, pp. 68–71, 2016.
- [14] U. Illahi, J. Iqbal, M. I. Sulaiman, M. M. Alam, M. M. Su'ud, and M. H. Jamaluddin, "Singly-fed rectangular dielectric resonator antenna with a wide circular polarization bandwidth and beamwidth for WiMAX/satellite applications," *IEEE Access*, vol. 7, pp. 66206–66214, 2019.
- [15] P. F. Hu, Y. M. Pan, K. W. Leung, and X. Y. Zhang, "Wide-/dual-band omnidirectional filtering dielectric resonator antennas," *IEEE Trans. Antennas Propag.*, vol. 66, no. 5, pp. 2622–2627, May 2018.

- [16] B. Li, C.-X. Hao, and X.-Q. Sheng, "A dual-mode quadrature-fed wide-band circularly polarized dielectric resonator antenna," *IEEE Antennas Wireless Propag. Lett.*, vol. 8, pp. 1036–1038, 2009.
- [17] M. Abedian, H. Oraizi, S. K. Abdul Rahim, S. Danesh, M. R. Ramli, and M. H. Jamaluddin, "Wideband rectangular dielectric resonator antenna for low-profile applications," *IET Microw., Antennas Propag.*, vol. 12, no. 1, pp. 115–119, Jan. 2018.
- [18] T. Kim and S. Pak, "Enhanced gain and miniaturisation method of stacked dielectric resonator antenna using metallic cap," *IET Microw., Antennas Propag.*, vol. 13, no. 8, pp. 1198–1201, Jul. 2019.
- [19] A. Kianinejad, Z. N. Chen, L. Zhang, W. Liu, and C.-W. Qiu, "Spoof plasmon-based slow-wave excitation of dielectric resonator antennas," *IEEE Trans. Antennas Propag.*, vol. 64, no. 6, pp. 2094–2099, Jun. 2016.
- [20] Z.-Y. Qian, W.-J. Sun, X.-F. Zhang, and J.-X. Chen, "An X-band magnetic dipole quasi-Yagi antenna based on a dielectric resonator," *Int. J. Microw. Wireless Technol.*, vol. 12, no. 3, pp. 240–245, Apr. 2020.
- [21] Z.-Y. Qian, L.-L. Yang, and J.-X. Chen, "Design of dual-/wide-band quasi-Yagi antenna based on a dielectric resonator," *IEEE Access*, vol. 8, pp. 16934–16940, 2020.
- [22] L. Yang and J. Zhuang, "Compact quasi-Yagi antenna with enhanced bandwidth and stable high gain," *Electron. Lett.*, vol. 56, no. 5, pp. 219–220, Mar. 2020.
- [23] B. Zhou and T. Jun Cui, "Directivity enhancement to Vivaldi antennas using compactly anisotropic zero-index metamaterials," *IEEE Antennas Wireless Propag. Lett.*, vol. 10, pp. 326–329, 2011.
- [24] G. Zhai, X. Wang, R. Xie, J. Shi, J. Gao, B. Shi, and J. Ding, "Gain-enhanced planar log-periodic dipole array antenna using nonresonant metamaterial," *IEEE Trans. Antennas Propag.*, vol. 67, no. 9, pp. 6193–6198, Sep. 2019.
- [25] A. Dadgarpour, B. Zarghooni, B. S. Virdee, and T. A. Denidni, "Millimeter-wave high-gain SIW end-fire bow-tie antenna," *IEEE Trans. Antennas Propag.*, vol. 63, no. 5, pp. 2337–2342, May 2015.
- [26] S. W. Wong, T. G. Huang, C. X. Mao, Z. N. Chen, and Q. X. Chu, "Planar filtering ultra-wideband (UWB) antenna with shorting pins," *IEEE Trans. Antennas Propag.*, vol. 61, no. 2, pp. 948–953, Feb. 2013.
- [27] X. Y. Zhang, W. Duan, and Y.-M. Pan, "High-gain filtering patch antenna without extra circuit," *IEEE Trans. Antennas Propag.*, vol. 63, no. 12, pp. 5883–5888, Dec. 2015.
- [28] G. Liu, Y. M. Pan, T. L. Wu, and P. F. Hu, "A compact planar quasi-Yagi antenna with bandpass filtering response," *IEEE Access*, vol. 7, pp. 67856–67862, 2019.
- [29] C.-H. Wu, C.-H. Wang, S.-Y. Chen, and C. H. Chen, "Balanced-to-unbalanced bandpass filters and the antenna application," *IEEE Trans. Microw. Theory Techn.*, vol. 56, no. 11, pp. 2474–2482, Nov. 2008.
- [30] K.-D. Xu, H. Xu, and Y. Liu, "Low-profile filtering end-fire antenna integrated with compact bandstop filtering element for high selectivity," *IEEE Access*, vol. 7, pp. 8398–8403, 2019.
- [31] F. Wei, X.-B. Zhao, and X. W. Shi, "A balanced filtering quasi-Yagi antenna with low cross-polarization levels and high common-mode suppression," *IEEE Access*, vol. 7, pp. 100113–100119, 2019.
- [32] H. Tang, J.-X. Chen, H. Chu, G.-Q. Zhang, Y.-J. Yang, and Z.-H. Bao, "Integration design of filtering antenna with load-insensitive multilayer balun filter," *IEEE Trans. Compon., Packag., Manuf. Technol.*, vol. 6, no. 9, pp. 1408–1416, Sep. 2016.
- [33] J. Shi, X. Wu, Z. N. Chen, X. Qing, L. Lin, J. Chen, and Z.-H. Bao, "A compact differential filtering quasi-Yagi antenna with high frequency selectivity and low cross-polarization levels," *IEEE Antennas Wireless Propag. Lett.*, vol. 14, pp. 1573–1576, 2015.



where she is currently a Lecturer. Her current research interest includes microwave antenna.



YAN-YUAN ZHU was born in Jiangsu, China. He received the B.S. and M.S. degrees from Nantong University, Nantong, China, in 2015 and 2018, respectively. He is currently pursuing the Ph.D. degree in electronic science and technology from the Nanjing University of Science and Technology, Nanjing, China.

His current research interests include microwave circuits, antennas, and millimeter-wave circuits.



JIANPENG WANG received the Ph.D. degree from the University of Electronic Science and Technology of China, Chengdu, China, in 2007. From 2005 to 2006, he was a Research Assistant with the Institute for Infocomm Research, Singapore. From 2010 to 2011, he was a Research Fellow with the School of Electrical and Electronic Engineering, Nanyang Technological University, Singapore. In 2013, he was a Visiting Scholar with the School of Engineering and Physical Sciences, Heriot-Watt University, Edinburgh, U.K. In 2014, 2016 and 2017, he was a Research Fellow with the Faculty of Science and Technology, University of Macau, Zhuhai, Macao. He is currently a Professor with the School of Electronic and Optical Engineering, Nanjing University of Science and Technology, Nanjing, China. He has authored or coauthored over 100 articles in international journals and conference proceedings. His current research interests include microwave circuits, antennas, and LTCC-based millimeter wave circuits. From 2015 to 2018, he was an Associate Editor of the *IET Electronics Letters*.



JIAN-XIN CHEN (Senior Member, IEEE) was born in Nantong, Jiangsu, China, in 1979. He received the B.S. degree from the Huaiyin Teachers College, Jiangsu, in 2001, the M.S. degree from the University of Electronic Science and Technology of China (UESTC), Chengdu, China, in 2004, and the Ph.D. degree from the City University of Hong Kong, Hong Kong, in 2008.

Since 2009, he has been with Nantong University, Jiangsu, where he is currently a Professor. He has authored or coauthored more than 80 internationally refereed journal and conference papers. He holds three Chinese patents and two U.S. patents. His research interests include microwave active/passive circuits and antennas and LTCC-based millimeter-wave circuits and antennas. He was a recipient of the Best Paper Award presented at the Chinese National Microwave and Millimeter-Wave Symposium, Ningbo, China, in 2007. He was a Supervisor of 2014 iWEM Student Innovation Competition Winner, Sapporo, Japan.



YAN-HUI KE was born in Wuxi, Jiangsu, China, in 1998. He received the B.S. degree from Nantong University, Nantong, China, in 2020, where he is currently pursuing the M.S. degree in electromagnetic field and microwave technology. His current research interests include filter and antenna.